

Complexity Project: The Oslo Model (python 3.6.4)

February 18, 2019

Abstract

The self-organised criticality of the Oslo model is explored by looking at the pile heights and avalanche-size probabilities ($P_N(s; L)$) using python 3.6.4. Pile heights were not Gaussian distributed and so the individual site slopes are not independent. Avalanche sizes span twelve orders of magnitude and so the system response is not always local and small. Data collapse for the $P_N(s; L)$ with exponents $\tau_s = 1.561$ and $D = 2.235$ were of good quality and agreed with exponents from moment analysis, which reveals that there is self-organised criticality in the Oslo model.

Introduction

In this project the aim is to explore self-organised criticality. In self-organising systems (complex systems), a set of simple rules are continuously applied to a system that give rise to emergent behaviour. Criticality is the behaviour of the whole system due to its constituent parts, where this behaviour could not be understood by simply considering the behaviour of a single entity in the system [1 - preface]. Performing a data collapse and checking for scaling will reveal whether the system is displaying self-organised criticality.

In the Oslo model, we define a one-dimensional lattice with length L and each site is one unit so there are L sites in the system. Each site has properties, a height h_i , a slope z_i and a threshold slope z_i^{th} where the slope is defined as $h_i - h_{i+1}$ and the threshold slope is randomly selected, $z_i^{th} = (0, 1)$. The system is initiated with empty sites ($h_i = 0$, for all i) and a random threshold slope for each site, then the system is continuously driven by adding a grain to the first site after the system is relaxed. The slope of each site is altered if it is greater than the threshold slope, this process is re-

laxation.

The system height and avalanche size will be explored in detail and compared to theoretical expectations. Data was collected for system sizes $L = 4, 8, 16, 32, 64, 128, 256$, with ten realisations for each system size because this smoothed out the data sufficiently. Each system was driven one hundred thousand times because this gave enough points for the largest system size $L = 256$ above its critical time t_c for the patterns to be observed.

1 Implementation of the Oslo model (1)

To test my implementation, the model was run with these five tests:

Test one: measure the average height over time ($\langle h \rangle$) for system size of sixteen, compare this to the given value of 26.5.

Test two: measure the $\langle h \rangle$ for system size of thirty-two, compare this to the given value of 53.9.

Test three: set the probability of each site

threshold slope (z_i^{th}) being one to one (so that z_i^{th} is always one) and you should observe the height of the steady-state pile is equal to the system size.

Test four: set the probability of each site threshold slope (z_i^{th} being two to one (so that z_i^{th} is always two) and you should observe the height of the steady-state pile is equal to twice the system size.

Test five: measure the critical time (the time it takes for the system to reach a steady state) t_c and check that it is equal to the sum of the heights of the sandbox sites.

These tests were passed as shown in figure 1, and they show that the implementation of the Oslo model is correct.

```
For threshold probability = 0.5 and L = 16:
Average height over time = 26.52997601918465

For threshold probability = 0.5 and L = 32:
Average height over time = 53.84190231362468

For L = 16 and probability = 1 of z threshold = 1:
Sum of heights = 136
Critical time = 136
Height = 16
Critical time is equal to the sum of heights of each site as expected.

For L = 32 and probability = 1 of z threshold = 1:
Sum of heights = 528
Critical time = 528
Height = 32
Critical time is equal to the sum of heights of each site as expected.

For L = 16 and probability = 1 of z threshold = 2:
Height = 32
Sum of heights = 272
Critical time = 272
Critical time is equal to the sum of heights of each site as expected.

For L = 32 and probability = 1 of z threshold = 2:
Height = 64
Sum of heights = 1056
Critical time = 1056
Critical time is equal to the sum of heights of each site as expected.
```

Figure 1: Tests carried out to check Oslo model is working correctly. The results are as expected for a working Oslo model.

2 The height of the pile

2.1 Pile heights over time (2a)

The height of the pile was defined to be the height of the first site in the system. Transient and recurrent configurations are the two types of stable configurations which the system enters as grains are added. A stable configuration is a configuration where all sites have been relaxed and so all

$z_i < z_i^{th}$. Transient configurations are only visited once and no transient configuration is entered by the system after the first recurrent configuration appears. When the average input of grains into the system equals the average grains leaving the system, the system is in a stable recurrent configuration, when the opposite is true then the system is in a transient configuration[1 - page 257].

The transient stable configurations can be seen to be the curved parts of the graphs in figure two. This is because the height of the pile is changing in the curved region which means that the average number of grains entering the system is not equal to the average number of grains leaving the system. The grains not leaving are contributing to increasing the height. Figure two shows that all of the transient parts of the each system size lie on the same graph. This is because the system behaves as if it is infinite and so the behaviour of the transient will be the same for all system sizes. This is because every system starts from an empty configuration and so has to pass through the same transient configurations until it reaches its finite system size recurrent configuration. When we limit the system size we cause the system to exit the transient at a critical time.

The flat line in figure two is the recurrent stable configuration because the height remains constant with minor fluctuations. Therefore, the grains that enter also leave the system not contributing to increasing the height. Each system size has a different requirement of the number of grains needed to reach a recurrent configuration. The minor fluctuations are due to selecting a threshold slope randomly.

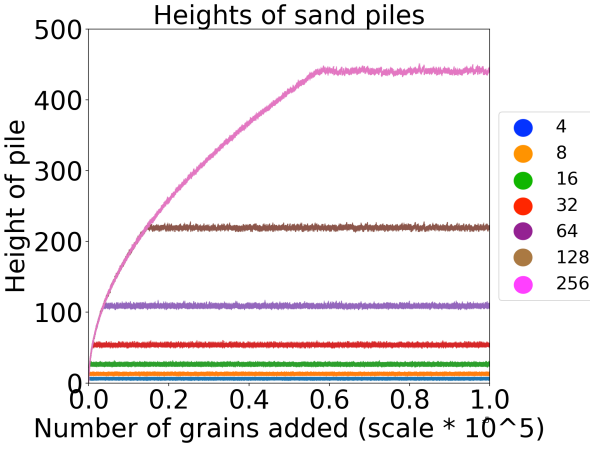


Figure 2: The height of each system size is shown as a function of the number of grains added. Transient region is the curved part and recurrent region is the flat line. All transient regions lie on the same curve, however the recurrent regions do not.

2.2 Scaling behaviour for $L \gg 1$ (2b)

For a large system ($L \gg 1$), the local behaviour about a site will be similar to the local behaviour at another site after the steady state has been reached. At the boundaries there be different behaviour, however these can be ignored for large system sizes. Therefore, the average local slope at one site can be assumed to be equal to the average local slope at other sites and so,

$$\langle z_i(t) \rangle = \langle z(t) \rangle, \quad (1)$$

which means we assume the average slope at any site to be the average slope of the pile $\langle z \rangle$.

Starting from the given expression for the height of the pile,

$$h(t, L) = \sum_{i=1}^L z_i(t), \quad (2)$$

and then taking the average over time and using the result from (1),

$$\langle h(t, L) \rangle = \left\langle \sum_{i=1}^L z_i(t) \right\rangle = \sum_{i=1}^L \langle z_i(t) \rangle,$$

$$\begin{aligned} \langle h(t, L) \rangle &= \sum_{i=1}^L \langle z_i(t) \rangle = \langle z(t) \rangle \sum_{i=1}^L 1, \\ \langle h(t, L) \rangle &= \langle z(t) \rangle L. \end{aligned} \quad (3)$$

Therefore, the height of the pile is directly proportional to the system size with the constant of proportionality being the average slope of the system.

Using this result the critical time can be shown to be proportional to L^2 . The critical time is defined as the time until the system enters the first recurrent configuration. When the system reaches the steady state it will have a height $h(t, L)$ and L sites. As before, we assume the average local slope to be the same for all sites and so the average system slope is the local average slope (equation 1). Therefore, the pile is now approximated as a triangle with area $\frac{h(t, L)L}{2}$, which corresponds to the critical time $t_c(L)$. One grain added to the system is a the measure of a unit of time, and every time a grain is added the system will relax all sites until all $z_i < z_i^{th}$. Therefore once the final site is relaxed, the grain will leave the system with all the sites in a stable configuration. This is the first recurrent configuration, so the number of grains in the pile at that moment is the critical time.

$$\langle t_c(L) \rangle = \frac{\langle h(t, L)L \rangle}{2} = \frac{\langle z(t) \rangle L^2}{2}. \quad (4)$$

2.3 Data collapse for the processed height \tilde{h} (2c)

A data collapse for the processed height $\tilde{h}(t, L)$ is performed by plotting each system size with the height and number of grains added scaled by a factor so that all data lie on the same graph.

From equation three, $\langle h(t, L) \rangle \propto L$, and so the height of each system was divided by L (figure four). This aligned the plots vertically because $\frac{\langle \tilde{h}(t, L) \rangle}{L} = \langle z(t) \rangle$, which means that the ratio of processed height to L will give a constant value which all plots will lie on. From equation four,

$\langle t_c(L) \rangle \propto L^2$. Therefore, the time was divided by the system size squared to align the plots horizontally so that the transition point from transient to recurrent configurations is aligned (figure five). This worked because $\frac{\langle t_c(L) \rangle}{L^2} = \frac{\langle z(t) \rangle}{2}$, which means that the ratio of critical time to L^2 will give a constant value which all plots lie on.

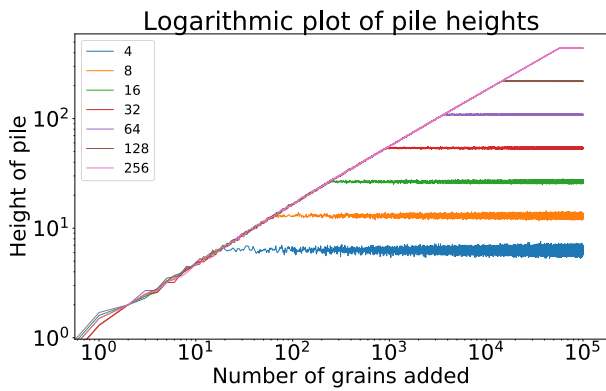


Figure 3: Unscaled graphs plotted on a logarithmic scale.

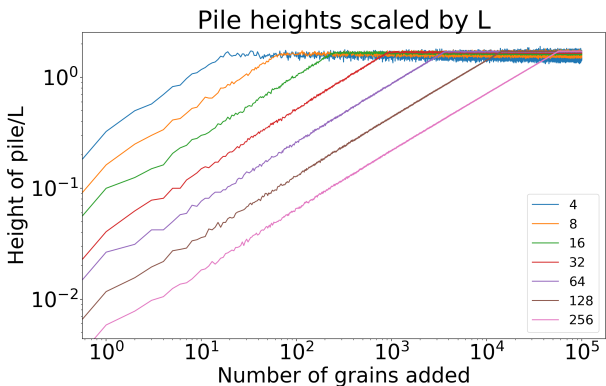


Figure 4: Height of each pile is scaled by dividing by the corresponding system size L . This aligns the plots vertically. The value they collapse to is about 1.71.

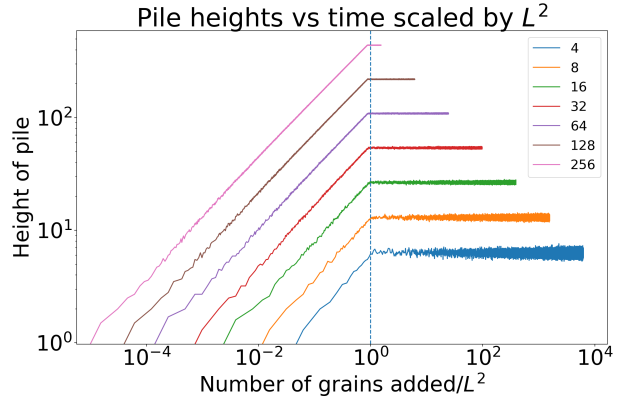


Figure 5: The number of grains added is scaled by dividing by L^2 to align the plots horizontally. Each scaled plot has its transition point from transient to recurrent configurations on the blue dotted line.

Combining the scaling of the height and time, the plots all collapse onto the same graph (figure six). Mathematically:

$$F : \tilde{h}(t, L) = \frac{1}{L} F\left(\frac{t}{L^2}\right), \quad (5)$$

where F is the scaling function, $\tilde{h}(t, L)$ is the processed height, t is the time and L is the system size. Figure six shows a good quality of data collapse and so there is strong evidence that the pile is exhibiting self-organised criticality.

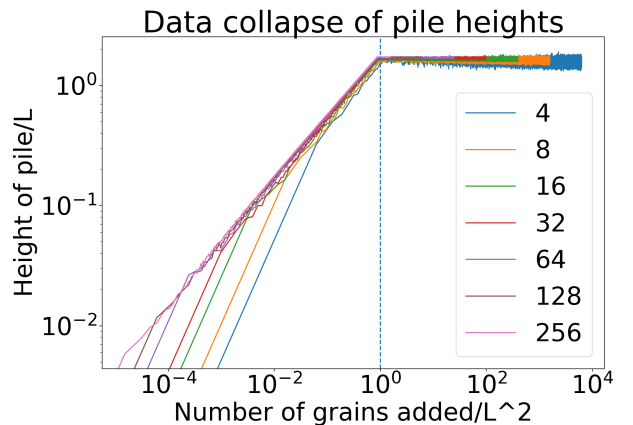


Figure 6: Data collapse of the processed height shows that the plots all lie on the same plot and so there is strong evidence for self-organised criticality. The vertical value of the line of collapse is about 1.71, and the horizontal value is about 1.

For $F\left(\frac{t}{L^2} \gg 1\right)$, figure six shows that there is a flat line. Therefore the scaling

function tends to a constant. This must be so because $t_c \propto L^2$. Using the fact that t_c is the time it takes for the system to enter the first recurrent configuration, it follows that for any time much greater than t_c the pile height should reach a steady value. This is because the average number of grains entering equals the average number of grains leaving the system.

For $F\left(\frac{t}{L^2} << 1\right)$, the line can be fitted to extract the gradient which is the exponent of the time t . From figure six, the gradient of the transient part is about equal to a half, so $\tilde{h}(t; L) \propto t^{0.5}$ during the transient. For the time that the system is passing through the transient configurations the number of grains entering the system is increasing. As these grains are toppled, the height of the pile is not expected to grow linearly but much slower. This is because the grains are being shifted to the right as they topple. Only after all the sites to the right of the first site build up so that the slope of the first site is less than z_i^{th} , there is an increase in the pile height.

2.4 Numerical and theoretical critical times (2d)

The average $t_c(L)$ value over ten realisations will be used and compared to the theoretical values. Starting from the definition of $t_c(L) = \sum_{i=1}^L z_i i$ and using the assumption $\langle z_i(t) \rangle = \langle z(t) \rangle$,

$$\begin{aligned} \langle t_c(L) \rangle &= \left\langle \sum_{i=1}^L z_i i \right\rangle = \sum_{i=1}^L \langle z_i i \rangle = \langle z \rangle \sum_{i=1}^L i, \\ \sum_{i=1}^L i &= \frac{L(L+1)}{2}, \\ \langle t_c(L) \rangle &= \langle z \rangle \frac{L(L+1)}{2} = \frac{\langle z \rangle L^2}{2} \left(1 + \frac{1}{L}\right). \end{aligned} \quad (6)$$

This is the theoretical $t_c(L)$. The average slope of the pile is calculated numerically: $\langle z \rangle = 1.71$. Define N_1 and N_2 as the number of sites with threshold slope one and

two respectively. Each threshold slope is selected randomly between one and two, the sites with threshold slope one will be more likely to topple when adding a grain because they require less grains to induce toppling. Define the rate R_1 and R_2 as the rate at which a site with threshold equal to the subscript topples. R_1 will be greater than R_2 because of reasons explained above. Now to calculate the average threshold, $\langle z \rangle = \frac{N_1 + 2N_2}{L}$, is used where $N_1 + N_2 = L$. This is true because the probabilities of a site being having either threshold slope is: $\frac{N_1}{N_1 + N_2}$, $\frac{N_2}{N_1 + N_2}$, respectively. Therefore, the expectation value of z gives $\frac{N_1}{N_1 + N_2} + \frac{2N_2}{N_1 + N_2}$.

Figure seven shows the percentage difference drops below 2% for systems above $L = 64$ and that as the system size increase the two values are in strong agreement. This is explained by the finite-sized corrections to scaling which come into play for all finite systems but are more noticeable for smaller systems. As $L \Rightarrow \infty$, $1 + \frac{1}{L} \Rightarrow 0$ and so $\langle t_c(L) \rangle \Rightarrow \frac{\langle z \rangle L^2}{2}$. This is the same result that was shown in equation four. Therefore, the smaller system sizes show a larger deviation from the theoretical value due to corrections to scaling being more prominent for smaller systems, and larger systems are closer to theoretical values because the corrections to scaling are smaller for larger systems.

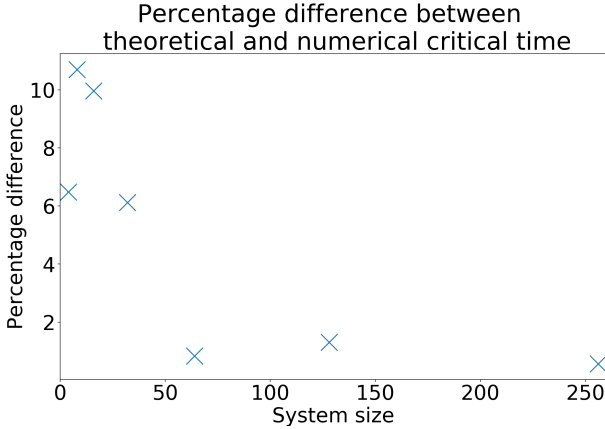


Figure 7: The percentage difference is shown to start at about 6.5% and peak at 11% before a rapid decay to values below 2%. This suggests that for large L the theoretical and numerical values are in strong agreement.

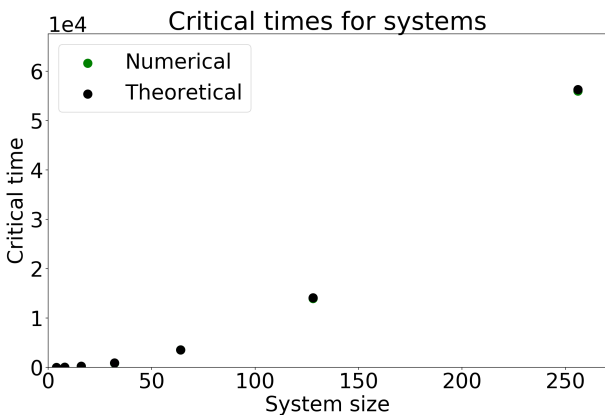


Figure 8: Numerical and theoretical critical times for different system sizes. The two values are close together and are difficult to distinguish visually.

2.5 Corrections to scaling for the average height (2e)

The correction to scaling form was assumed to be,

$$\langle h(t, L) \rangle = a_0 L (1 - a_1 L^{-\omega_1} + a_2 L^{-\omega_2} + \dots),$$

where a_i are constants and $\omega_i > 0$.

The average height was calculated using,

$$\langle h(t; L) \rangle_t = \lim_{T \rightarrow \infty} \frac{1}{T} \sum_{t=t_0+1}^{T+t_0} h(t; L),$$

where $t_0 > t_c$.

Neglecting terms above ω_1 , the expression for $\langle h(t, L) \rangle$ reduces to $a_0 L (1 - a_1 L^{-\omega_1})$. Re-arranging and taking the natural logarithm of both sides, the equation can be cast into the form $y = mx + c$:

$$\ln \left(1 - \frac{\langle h(t, L) \rangle}{a_0 L} \right) = \ln(a_1) - \omega_1 \ln(L), \quad (7)$$

where the intercept $c = \ln(a_1)$ and the gradient $m = -\omega_1$.

To extract a_0 and ω_1 , the left hand side of equation seven was plotted against $\ln(L)$ for a range of a_0 values as this will produce a straight line which allows the exponents to be extracted by fitting the data. As the argument of a logarithm must be greater than zero, $a_0 > \frac{\langle h(t, L) \rangle}{L}$. Theoretically, this should be greater than $\langle z(t) \rangle = 1.71$ (using equation 3 and result for $\langle z(t) \rangle$ from section 2.4). Then multiple data sets were produced with different values of a_0 and each was fitted with a straight line. The linear regression value (r-value) was plotted for each a_0 and then the maximum r-value was calculated as the best linear fit corresponds to the r-value closest to one. The corresponding a_0 value was found to be $a_0 = 1.737 \pm 0.007$. This a_0 value gave the best fit to a straight line for equation seven. Using the gradient corresponding to this a_0 value, the value of ω_1 was calculated to be $\omega_1 = 0.540 \pm 0.008$.

a_0 is larger than the theoretical value by 1.5% and so they are in agreement. Therefore, the value of ω_1 is close to the true value. These results show that there are corrections to scaling to the pile height. For large values of L the corrections to scaling decay quickly due to the exponent of $L^{-0.54}$ being negative and less than one. For smaller L the corrections to scaling will be more visible.

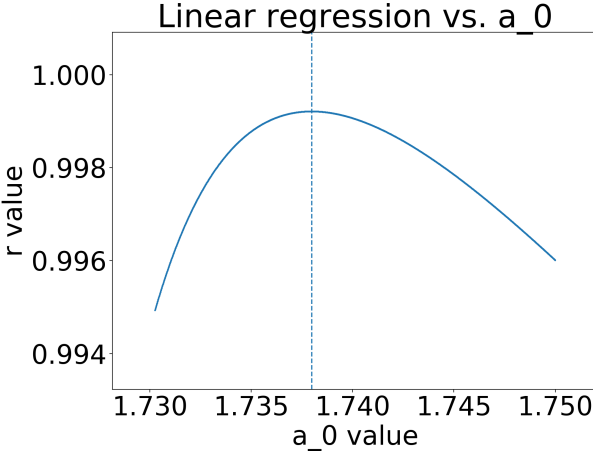


Figure 9: Linear regression is plotted against the a_0 value. The value of a_0 which maximises r is $a_0 = 1.737 \pm 0.007$ and is the blue dotted line.

2.6 Standard deviation of height (2f)

The central limit theorem states that as the number of independent and identically distributed random variables tends to infinity the distribution can be approximated as Gaussian. Therefore the height of the pile for each system size is assumed to be distributed about a mean value $\langle h \rangle$ with a spread σ_h , as a Gaussian. This is because we are taking $L \gg 1$. Using the central limit theorem, $\sigma_h^2 \propto \frac{1}{N}$, so $\frac{\sigma_h^2}{L^2} \propto \frac{1}{L}$. This shows that the expected relation for a Gaussian distributed height should give $\sigma_h \propto L^{0.5}$.

To check the actual relation between σ_h and L , the relation $\sigma_h \propto L^\alpha$ was plotted on a logarithmic scale. The standard formula for the standard deviation was used to calculate σ_h ,

$$\sigma_h(L) = \sqrt{\langle h^2(t; L) \rangle_t - \langle h(t; L) \rangle_t^2}.$$

The exponent α was extracted from the gradient of a straight line fit as $\ln(\sigma_h) \propto \alpha \ln(L)$ and is shown in figure ten.

The value for the exponent of L was found to be $\alpha = 0.248 \pm 0.003$, where the error was calculated using the python 'polyfit'

function, so $\sigma_h(L) \propto L^{0.248}$. This value of α does not match the exponent of the Gaussian distributed σ_h , therefore the height of the pile after the critical time is not a Gaussian distribution. The reason behind this is related to the two threshold slopes. As explained in section 2.4, R_2 is less than R_1 and so the first site will spend more time with a slope of two then in a slope of one. This will skew the data away from Gaussian.

From section 2.5, $\langle h(t, L) \rangle = a_0 L (1 - a_1 L^{-w_1})$. Taking the limit $L \Rightarrow \infty$, $\langle h(t, L) \rangle \Rightarrow a_0 L$, therefore $\langle z \rangle \Rightarrow a_0$, and so $\langle z \rangle \Rightarrow 1.737$. The standard deviation of the average slope will be proportional to the scaled standard deviation of the average height, $\sigma_z \propto \frac{\sigma_h}{L}$. Then using the result for σ_h , the standard deviation of the average slope is $\sigma_z \propto \frac{L^{0.248}}{L} = L^{-0.752}$. Therefore, as $L \Rightarrow \infty$, $\sigma_z \Rightarrow 0$. This implies that the slope will tend to a constant value with no deviations as $L \Rightarrow \infty$.

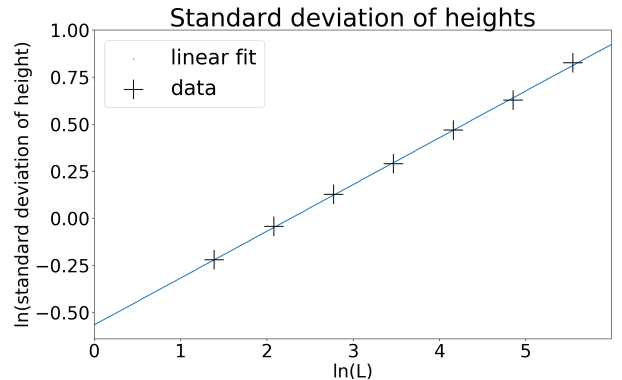


Figure 10: Straight line fit of the logarithm of standard deviations and system size.

2.7 Height probability (2g)

Theoretically, the probability of height h in a system size L , $P(h; L)$, is expected to be distributed as a Gaussian distribution when $L \gg 1$. This is because the z_i are assumed to be independent and identically distributed random variables and under central limit theory, the distribution of these z_i should tend to a Gaussian as the number of sites tends to infinity. Figure eleven shows the distributions of $P(h; L)$.

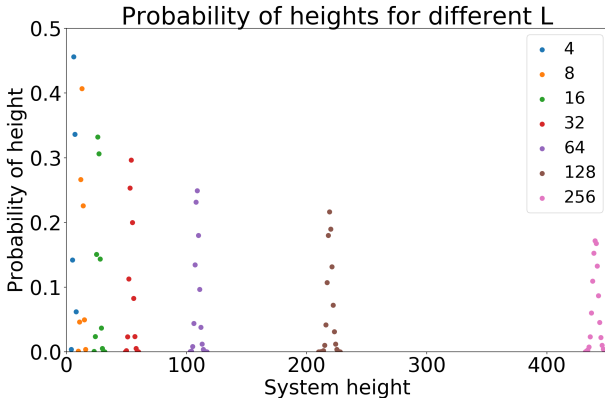


Figure 11: The average system height increases with increasing L . Each distribution peak decreases with increasing L .

To perform a data collapse of $P(h; L)$, the peak probability and the average system height of each distribution will need to be collapsed onto the same value. Using the assumption that $P(h; L)$ is a Gaussian, it will be of the form,

$$P(h; L) = \frac{1}{\sigma_h \sqrt{2\pi}} e^{\frac{1}{2} \left(\frac{h - \langle h \rangle}{\sigma_h} \right)^2},$$

therefore, if we let $x = \frac{h - \langle h \rangle}{\sigma_h}$, and multiply $P(h; L)$ by σ_h we get the normal distribution,

$$\sigma_h P(h; L) = \frac{1}{\sqrt{2\pi}} e^{\frac{1}{2}x^2},$$

which has mean equal to zero and a standard deviation equal to one. The probability was scaled by multiplying P_h by σ_h , as this aligned the peaks of the distributions.

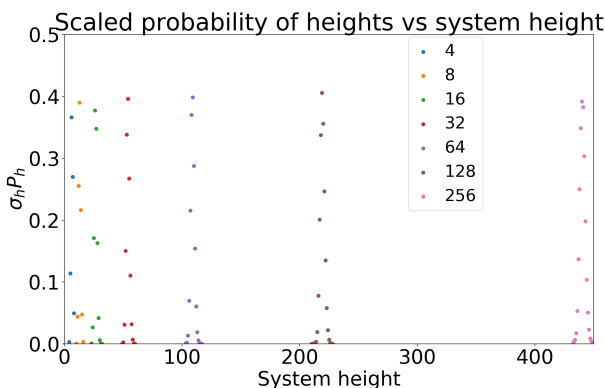


Figure 12: Scaled probability aligns the peaks of each distribution.

The height was scaled by $\frac{h - \langle h \rangle}{\sigma_h}$, because this aligned the averages of the distributions to zero.

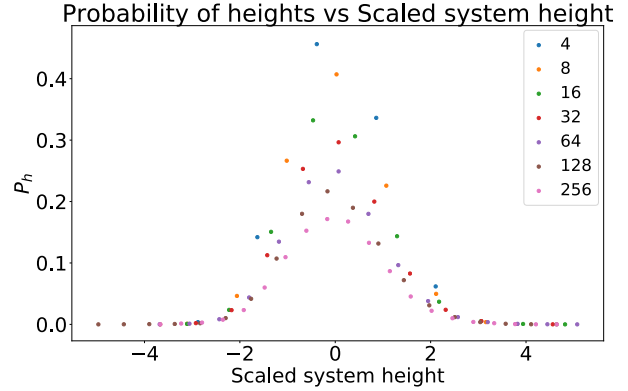


Figure 13: Scaled height of each distribution aligns the plots horizontally.

Figure fourteen shows that the data collapse traces out a distribution which is approximately Gaussian with mean equal to zero and standard deviation equal to one.

The assumption that z_i are independent, identically distributed random variables with finite variance produces a scaling of $\sigma_h(L) \propto L^{0.5}$. This is due to the central limit theorem and is explained in the first paragraph of section 2.6. Comparing this to the result from section 2.6, the individual distributions were shown to not be Gaussian as it was shown that $\sigma_h(L) \propto L^{0.248}$. Figure fourteen shows that the distributions collapse onto an approximate Gaussian but it is not Gaussian. This implies that the z_i are not independently distributed.

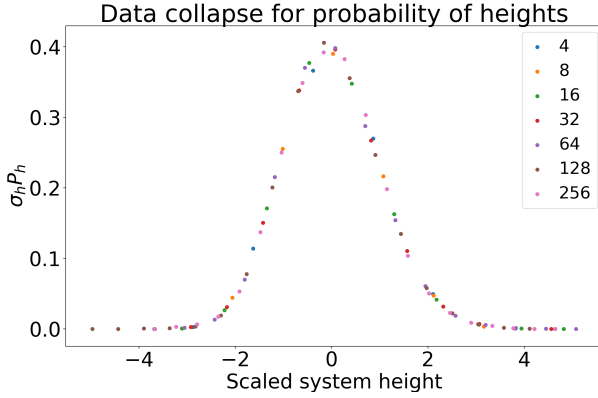


Figure 14: Data collapse for $P(h; L)$ shows an approximately Gaussian distribution with mean equal to zero and standard deviation equal to one.

3 Avalanche-size probabilities

3.1 Avalanche-size probabilities using log-binning (3a)

An avalanche size s is defined as the number of topples that occur after the system is driven and until all sites are relaxed. Avalanches after t_c are considered. The normalised avalanche size probability, $P_N(s; L)$, is equal to the number of avalanches of size s in a system of size L divided by the total number of avalanches in that system.

The data set is finite and so data binning can be used to extract the finite cut-off from the noisy tail (figure fifteen). Each bin spans $[a^j, a^{j+1}]$ and this bin length will increase exponentially for $a > 1$, and so the statistics in each bin will be of similar amounts [1 - appendix E]. $a = 1.65$ was chosen for log-binning because this reduced the noise sufficiently whilst keeping enough information to show the trend of $P(s; L)$.

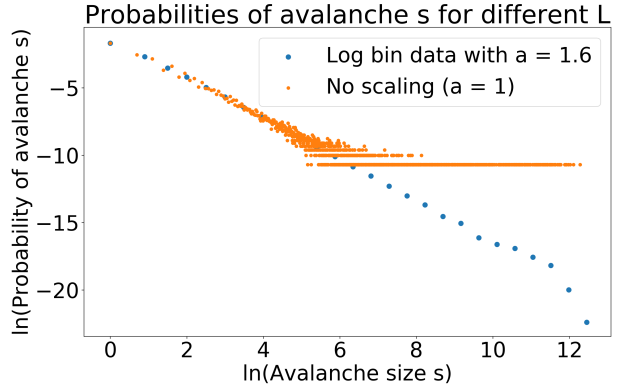


Figure 15: The underlying $P(s; L)$ is shown with the raw data.

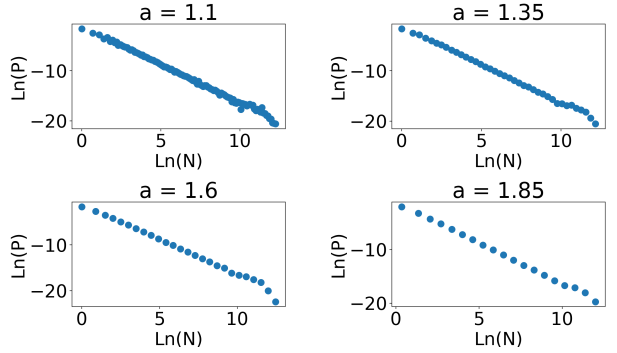


Figure 16: a values for log binning data for $L = 256$ are plotted. $a = 1.1$ is very noisy, then as a increase the noise is reduced whilst the trend remains clear.

There is a cut-off avalanche size s_c for each L (figure seventeen). All $P(s; L)$ exhibit the same behaviour before s_c , as they all lie on the same graph before s_c . There is also a bump in the data just before s_c . In addition, there is no typical s . The magnitude of s spans twelve orders of magnitude for $L = 256$. This means that the addition of one grain could cause a very small or huge avalanche. Therefore, the response of the system is not limited to be localised and small which means it is critical. However, avalanches of large magnitude are very unlikely. This is because each system behaves as if it is an infinite system which is why all $P(s; L)$ exhibit the same behaviour before s_c . Thus, the avalanche size diverges as $L \Rightarrow \infty$. When we limit the system size we get the finite-sized cut-off effect where avalanche sizes above s_c are exponentially unlikely to occur. We cannot

observe events above this imposed limit and so these $L \Rightarrow \infty$ events are squeezed in just before s_c when the system realises it is not infinite. Also, near s_c , the number of avalanches size s , N_s is over-represented because there are more combinations to give N_s near s_c . These are the reasons for the bump.

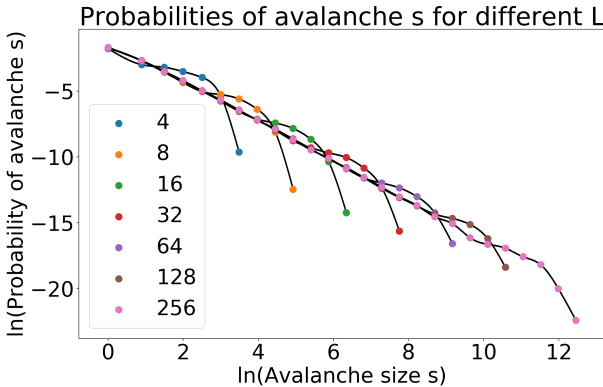


Figure 17: The logarithmic plot of $P(s; L)$ shows that there is a cut-off avalanche size s_c which is different for each system size. There is a bump just before s_c . Also, all $P(s; L)$ lie on the same plot before any cut-off.

3.2 Data collapse for avalanche-size probability (3b)

To test whether $P(s; L)$ are consistent with the finite-sized scaling ansatz,

$$\tilde{P}_N(s; L) \propto s^{-\tau_s} G\left(\frac{s}{L^D}\right), \quad (8)$$

where G is the scaling function, a data collapse was performed for $P(s; L)$.

Data collapse exponents τ_s, D were visually determined. Values were plotted from zero to five initially to check the behaviour, and then the values were altered accordingly. Aligned the tails as shown in figure eighteen, by altering τ_s and then lined up the cut-off parts by altering D as shown in figure nineteen. Figure nineteen shows a clean data collapse as all points lie on a well defined graph, apart from some minor fluctuation before the bump. This shows that $P(s; L)$ are consistent with the finite-scaling

ansatz in equation eight. The critical exponents which produced the best data collapse were $\tau_s = 1.561$ and $D = 2.235$ for $L \gg 1$.

Scaling ansatz assumes $L \gg 1$ to safely ignore corrections to scaling, so using system sizes of four, eight and sixteen was not sensible (figure twenty and twenty-one). They do not collapse well with the large system sizes due to corrections to scaling. Figure twenty shows that for the same exponents which produce a good data collapse for $L > 16$, the lower system sizes do not align. The best value for all system sizes was found to be $D = 2.08$. This data collapse (figure twenty-one) is not as good as in figure nineteen and so the finite-scaling ansatz is not true for small systems.

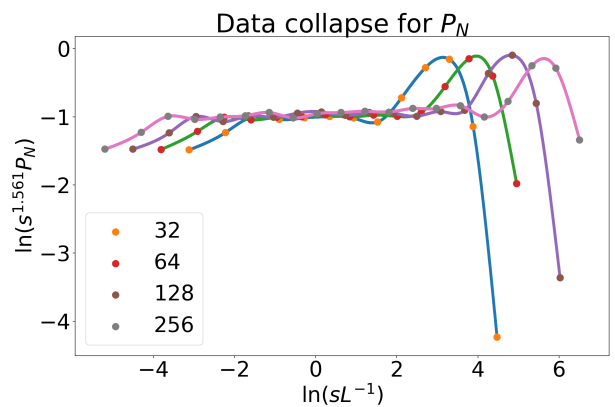


Figure 18: An interpolating function was used to fit a polynomial to the data. It can be seen that the tails align horizontally for the scaling of $P_N(s; L)$. System sizes above thirty-two plotted and others ignored due to corrections to scaling.

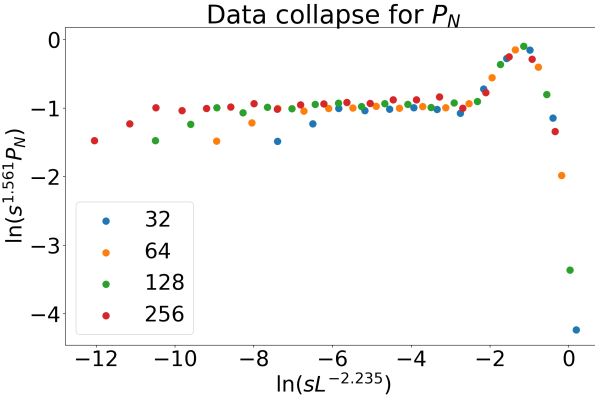


Figure 19: The complete data collapse with exponents $\tau_s = 1.561, D = 2.235$ show that the tails lie on minus one and the cut-off is around zero on this logarithmic plot. A bump is apparent just before the cut-off and the tail ends decrease exponentially.

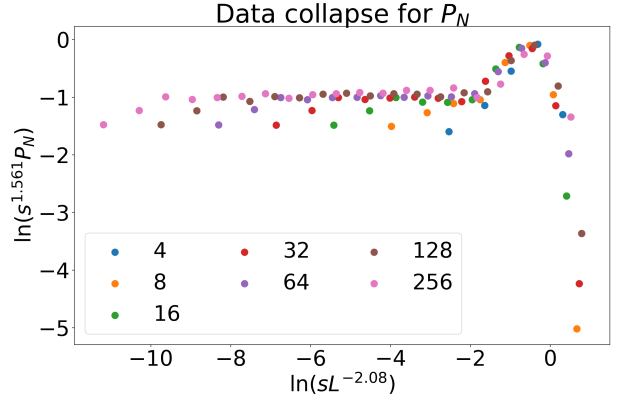


Figure 21: Complete data collapse with exponents $\tau_s = 1.561, D = 2.08$ including system size four, eight and sixteen. For $D = 2.08$ the data for smaller L lies on a similar graph to the larger L . However, there is more spread in the data collapse.

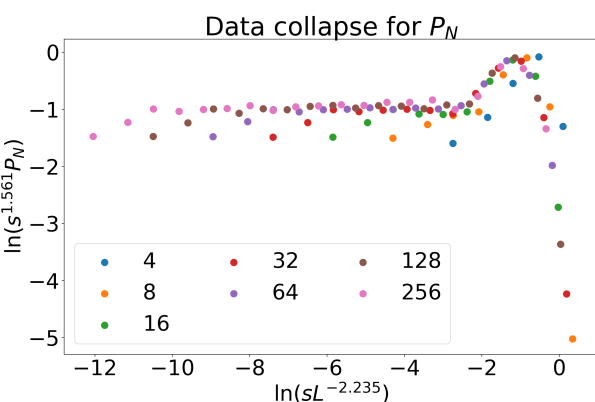


Figure 20: Complete data collapse with exponents $\tau_s = 1.561, D = 2.235$ including system sizes four, eight and sixteen. For $L = 4$, there is a very large difference compared to the larger system sizes. $L = 8$ is closer but still there is a visual difference, and $L = 16$ fits in much more than four and eight.

3.3 Moment scaling analysis (3c)

The k^{th} moment, $\langle s^k \rangle$, was calculated using its definition,

$$\langle s^k \rangle = \lim_{T \rightarrow \infty} \frac{1}{T} \sum_{t=t_0+1}^{T+t_0} s_t^k. \quad (9)$$

This is the expectation value of s^k which is also given by,

$$\langle s^k \rangle = \sum_{s=1}^{\infty} s^k P_N(s; L).$$

Inserting the finite-size scaling ansatz from equation eight,

$$\langle s^k \rangle = \sum_{s=1}^{\infty} s^{k-\tau_s} F\left(\frac{s}{L^D}\right).$$

Assuming equation eight is true for all s and approximating the sum as an integral over ds ,

$$\langle s^k \rangle \propto \int_1^{\infty} s^{k-\tau_s} F\left(\frac{s}{L^D}\right) ds.$$

Using a substitution of variables $u = \frac{s}{L^D}$, and setting the lower limit $\frac{1}{L^D} \Rightarrow 0$ as $L \gg 1$,

$$\langle s^k \rangle \propto L^{D(1+k-\tau_s)} \int_1^{\infty} u^{k-\tau_s} F(u) du$$

The integral will converge to a value in the lower limit if $t_s < 1 + k$, also in the upper limit the integral converges because the scaling function $F(u)$ decays fast enough. Therefore, the integral is simply a number and so,

$$\langle s^k \rangle \propto L^{D(1+k-\tau_s)}. \quad (10)$$

The exponents can also be extracted using moment scaling analysis of $P(s; L)$, which allow for the quantifying of errors on the exponents [2-page 99]. Taking the logarithm of both sides of equation ten and then plotting $\ln(\langle s^k \rangle)$ against $\ln(L)$ we obtain estimates for $D(1 + k - \tau_s)$ from the gradients for $k = 1, 2, 3, 4$. Then $D(1 + k - \tau_s)$ is plotted against k , a linear fit is applied to extract τ_s using the k -intercept and D is the gradient of this fitted line.

Using figure twenty-three, the k -intercept is at $k = \tau_s + 1$, so using the k -intercept the exponent value $\tau_s = 1.54 \pm 0.06$. The slope is equal to D , so $D = 2.13 \pm 0.09$. Comparing this τ_s to the value obtained from the data collapse of $P_N(s; L)$, it is a close match with a percentage difference of 1.4%. The value of D from moment scaling analysis has a percentage difference of 2.4% compared to the data collapse which includes the small system sizes. This in contrast to a difference of 4.9% to the data collapse with $L > 16$. This is because $L < 16$ have been included in the moment scaling analysis. However, when doing the moment scaling analysis with $L > 16$ as shown in figure twenty-four, the k -intercept is $\tau_s - 1 = 0.563$, therefore $\tau_s = 1.563$ and $D = 2.237$ to three s.f. This is in excellent agreement to two s.f. with the data collapse for $L > 16$. Therefore, the exponents get closer to the best data collapse values when we remove $L < 32$, this is evidence that there are corrections to scaling in the numerical data for the moments and that they are more significant for the lower L .

To further demonstrate the corrections to scaling, $\langle s \rangle / L$ vs $L^{D(2-\tau_s)} / L$ can be plotted for $k = 1$. This should be equal to one as

$\langle s \rangle = L$, because in the recurrent configuration a grain will topple around the order L times to leave the pile. Figure twenty-five shows that the value of $\langle s \rangle / L$ converges to one as L increases. This shows that there are corrections to scaling and that they are more prominent for smaller L and have to be considered more when dealing trying to obtain more precise measurements for the exponents [3-Conclusion].

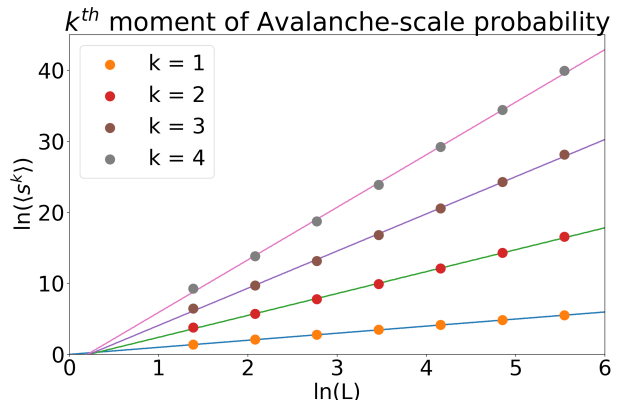


Figure 22: Moment analysis for $k = 1, 2, 3, 4$ is shown. Each plot lies on a straight line in log space where the $\ln(\langle s^k \rangle)$ increases linearly with $\ln(L)$.

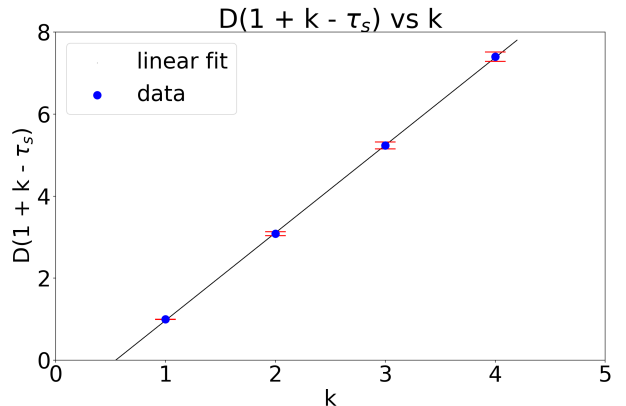


Figure 23: The exponent $D(1 + k - \tau_s)$ is plotted against k , using all L , revealing a linear fit. Error bars are also shown to increase with k . Exponents extracted from this are $\tau_s = 1.54 \pm 0.06$ and $D = 2.13 \pm 0.09$.

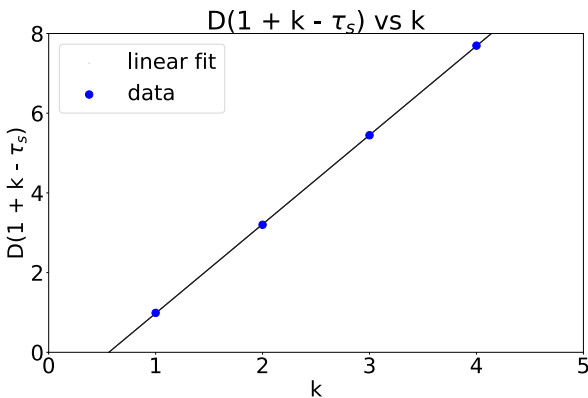


Figure 24: The exponent $D(1 + k - \tau_s)$ is plotted against k , using $L > 16$, revealing a linear fit. Exponents extracted from this are $\tau_s = 1.563$ and $D = 2.237$.

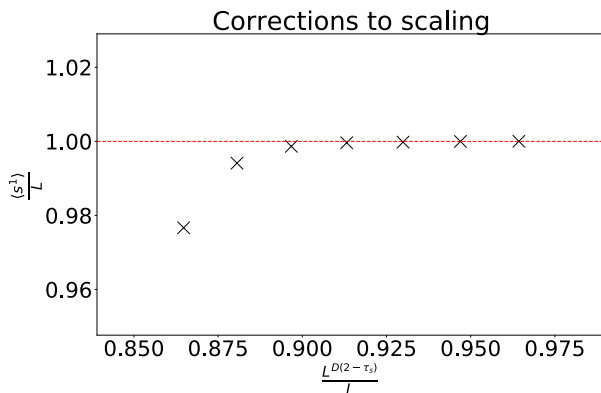


Figure 25: $\langle s \rangle / L$ is plotted against $L^{D(2 - \tau_s)}/L$ and a red dotted line is $y = 1$. For low L there are deviations from the known value of one with the largest being around 2%. The deviation for the next point is 0.5% and then there is a very close match for larger L .

Conclusion

The Oslo model has been shown to exhibit self-organising criticality because of the data collapses performed for the height and avalanche-size probabilities. The data collapse values were in full agreement with the moment analysis. System responses for avalanche-sizes were shown to vary by twelve orders of magnitude, meaning that the response to a single grain is not local or small. All system sizes behave in the same way before their cut-off point, which is due

to the finite-sized systems. Height distributions after the critical time were shown to be non-Gaussian which implied that the individual site slopes are not independent. The average slope of the pile was shown to tend to 1.737 and its standard deviation tends to zero as the system size tends to infinity. So, in an infinite system all slopes are equal after the critical time. Corrections to scaling were apparent in the height and moments. These corrections to scaling were more prominent for smaller system sizes, and for larger systems, the corrections to scaling converge to one.

References

- [1] K. Christensen and N.R. Moloney, Complexity and Criticality, ICP (2005).
- [2] G. Pruessner, Self-organised Criticality, Cambridge University Press (2012).
- [3] H. G. Ballesterosa, L. A. Fernandez, V. Martín-Mayor et al., Scaling corrections: site-percolation and Ising model in three dimensions, May 14, 1998.